

MODIS DATA STUDY TEAM PRESENTATION

October 27, 1989

AGENDA

1. Update on MODIS-N and -T Data Rates and Volumes
2. Delineation of the Roles of MODIS-N and -T in the Ocean Core Data Product Processing Scenario
3. Processing Overview for MODIS Land Data Products
4. MODIS Spectral Bands Required in the Ocean Data Processing Scenario
5. Sea Ice Determination By AVHRR as an Analogy to MODIS
6. Cloud Products Overview and Cloud Flag Setting Strategy for MODIS
7. Typical MODIS Radiances Over Land
8. Refined, but Still Preliminary, MODIS Core Data Product Accuracy Estimates
9. External Data Sets, External Look-Up Tables, and Internal Data Sets Required for MODIS Ocean Data Processing

Table 1. MODIS-N and MODIS-T Spectral and IFOV Parameters¹

MODIS-T Channel Parameters				MODIS-N Channel Parameters			
Band	Center Wavelength (nm)	IFOV (m)	Center Wavelength (μm)	Band	Center Wavelength (nm)	IFOV (m)	Center Wavelength (μm)
1	410	1,100	0.410	1	659	214	0.659
2	425	1,100	0.425	2	865	214	0.865
3	440	1,100	0.440	3	470	428	0.470
4	455	1,100	0.455	4	555	428	0.555
5	470	1,100	0.470	5	1240	428	1.240
6	485	1,100	0.485	6	1640	428	1.640
7	500	1,100	0.500	7	2060	428	2.060
8	515	1,100	0.515	8	2130	428	2.130
9	530	1,100	0.530	9	415	856	0.415
10	545	1,100	0.545	10	443	856	0.443
11	560	1,100	0.560	11	490	856	0.490
12	575	1,100	0.575	12	531	856	0.531
13	590	1,100	0.590	13	565	856	0.565
14	605	1,100	0.605	14	653	856	0.653
15	620	1,100	0.620	15	681	856	0.681
16	635	1,100	0.635	16	745	856	0.745
17	650	1,100	0.650	17	865	856	0.865
18	665	1,100	0.665	18	908	856	0.908
19	680	1,100	0.680	19	936	856	0.936
20	695	1,100	0.695	20	950	856	0.950
21	710	1,100	0.710	21	3750	856	3.750
22	725	1,100	0.725	22	3959	856	3.959
23	740	1,100	0.740	23	4050	856	4.050
24	755	1,100	0.755	24	4465	856	4.465
25	770	1,100	0.770	25	4515	856	4.515
26	785	1,100	0.785	26	4565	856	4.565
27	800	1,100	0.800	27	6715	856	6.715
28	815	1,100	0.815	28	7325	856	7.325
29	830	1,100	0.830	29	8550	856	8.550
30	845	1,100	0.845	30	9730	856	9.730
31	860	1,100	0.860	31	11030	856	11.030
32	875	1,100	0.875	32	12020	856	12.020
				33	13335	856	13.335
				34	13635	856	13.635
				35	13935	856	13.935
				36	14235	856	14.235

¹Channel information valid as of 10/25/89, as received by Bill Barnes/GSFC Code 564.

Table 2. MODIS-N and MODIS-T Data Rate and Volume Estimates²

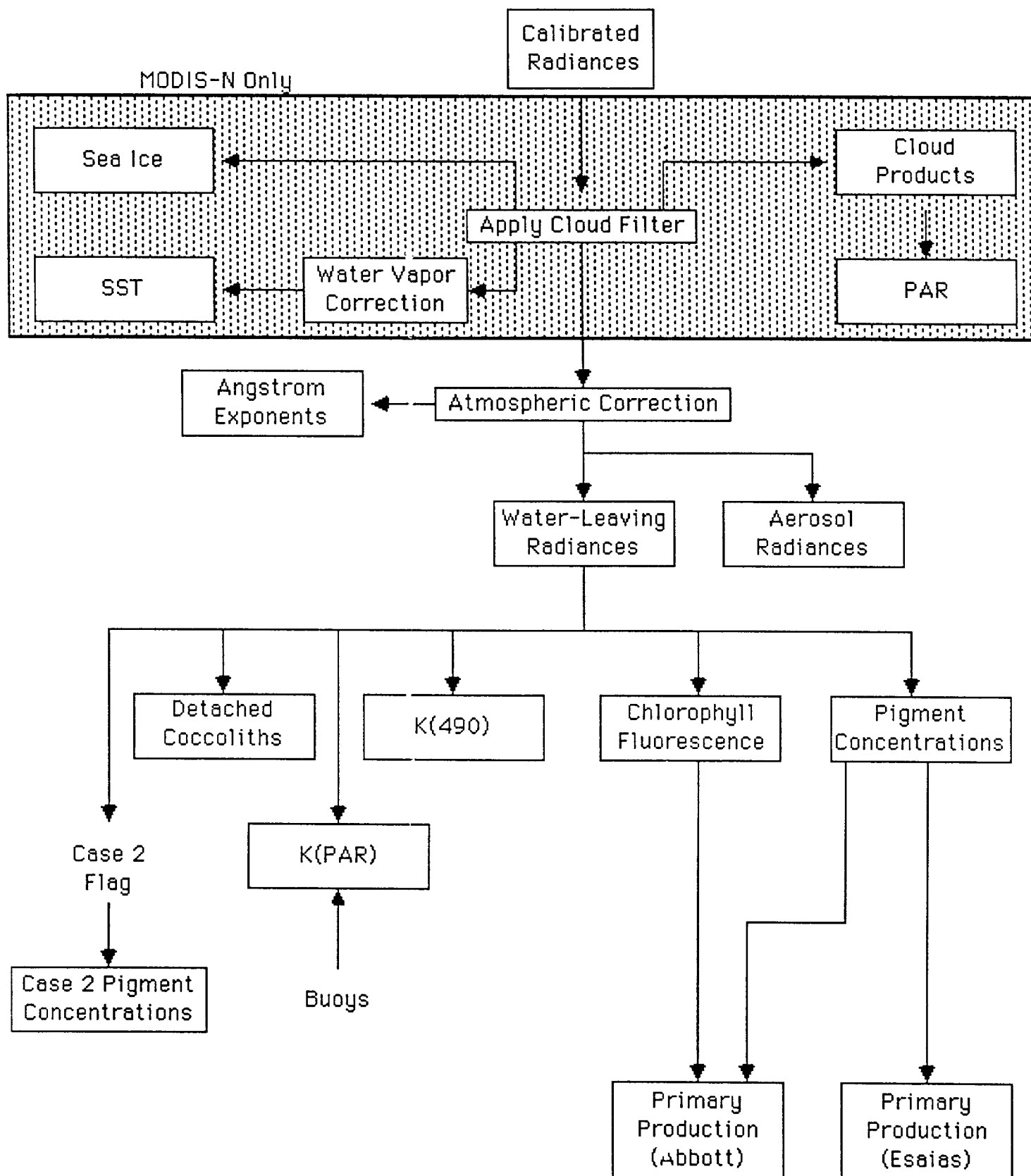
Earth Radius (km)	6371		
Satellite Altitude (km)	705		
Orbital Period (min)	98.9		
MODIS-N # 856 m REF channels	12		
MODIS-N # 428 m REF channels	6		
MODIS-N # 214 m REF channels	2		
MODIS-N # 856 m TIR channels	16		
MODIS-T # 1 km REF channels	32		
MODIS-N # bits/REF channel	12		
MODIS-N # bits/TIR channel	12		
MODIS-T # bits/REF channel	12		
MODIS-N REF Duty Cycle	50%		
MODIS-N TIR Duty Cycle	100%		
MODIS-T REF Duty Cycle	50%		
MODIS-N # Along-track IFOVs	8		
MODIS-T # Along-track IFOVs	32		
MODIS-N # Along-track detectors	672		
MODIS-T # Along-track detectors	32		
MODIS-N Maximum scan angle (deg)	55		
MODIS-T Maximum scan angle (deg)	45		
MODIS-N IFOV FWHM (deg)	6.95E-02		
MODIS-T IFOV FWHM (deg)	8.13E-02		
MODIS-N # pixels along-scan/on-Earth	1582		
MODIS-T # pixels along-scan/on-Earth	1107		
MODIS-N Scan Period (sec)	1.02		
MODIS-T Scan Period (sec)	4.75		
MODIS-N VIS Data (megabits/scan)	10.3		
MODIS-N TIR Data (megabits/scan)	2.4		
MODIS-N Daytime Data (megabits/scan)	12.8		
MODIS-T Daytime Data (megabits/scan)	13.6		
MODIS-N # Scans/Orbit	5841	Contingency	
MODIS-T # Scans/Orbit	625	10% Total	
MODIS-N Daytime Data Rate (mbps)	12.6	1.3	13.8
MODIS-N Nighttime Data Rate (mbps)	2.4	0.2	2.6
MODIS-T Daytime Data Rate (mbps)	2.9	0.3	3.2
MODIS-N Orbital Ave Data Rate (mbps)	7.5	0.7	8.2
MODIS-T Orbital Ave Data Rate (mbps)	1.4	0.1	1.6
MODIS-N Daily Data Volume (gigabits)	645.7	64.6	710.3
MODIS-T Daily Data Volume (gigabits)	123.8	12.4	136.2
Total MODIS Data Volume (gigabits)	769.6	77.0	846.5

² The parameters used in developing these estimates depend on the design of the MODIS-N and MODIS-T instruments and are therefore subject to change. Given the spectral band information provided in Table 1, the estimates are probably valid to $\pm 10\%$.

Delineation of the Roles of MODIS-N and T in the Ocean Core Data Product Processing Scenario

MODIS-N and T have different spectral complements and radiometric sensitivity. The core ocean data products they can generate will thus differ. In general, products requiring thermal infrared channels will only be produced by MODIS-N. These are sea ice, sea surface temperature, and photosynthetically active radiation estimates from clouds. However, both MODIS-N and T have the ability to generate the remaining ocean products. In the core data product processing scenario we present here (Figure 1), both sensors will generate water-leaving radiances and the products derived therefrom. This scenario produces redundancy in data products, but the tilt capability of MODIS-T will allow it to avoid sun glitter, while MODIS-N can provide coverage while T is changing its tilt. Furthermore, the reduced radiometric sensitivity of MODIS-N relative to T will probably enable it to recover more quickly from bright targets (land or clouds), thus allowing coverage where MODIS-T cannot. Duplicate processing will maximize spatial coverage and facilitate quality control. The products will most likely be combined for the production of Level 3 products.

MODIS N and T Ocean Core Data Product Processing Scenario



PROCESSING OVERVIEW FOR MODIS LAND DATA PRODUCTS

To avoid redundant generation of atmospheric products and improve overall data system efficiency, all atmospheric parameters required to correct MODIS observations for the effect of the atmosphere are best generated as stand-alone atmospheric products. Processing to generate MODIS land products then includes only those processing steps specifically needed to generate land products given known atmospheric characteristics.

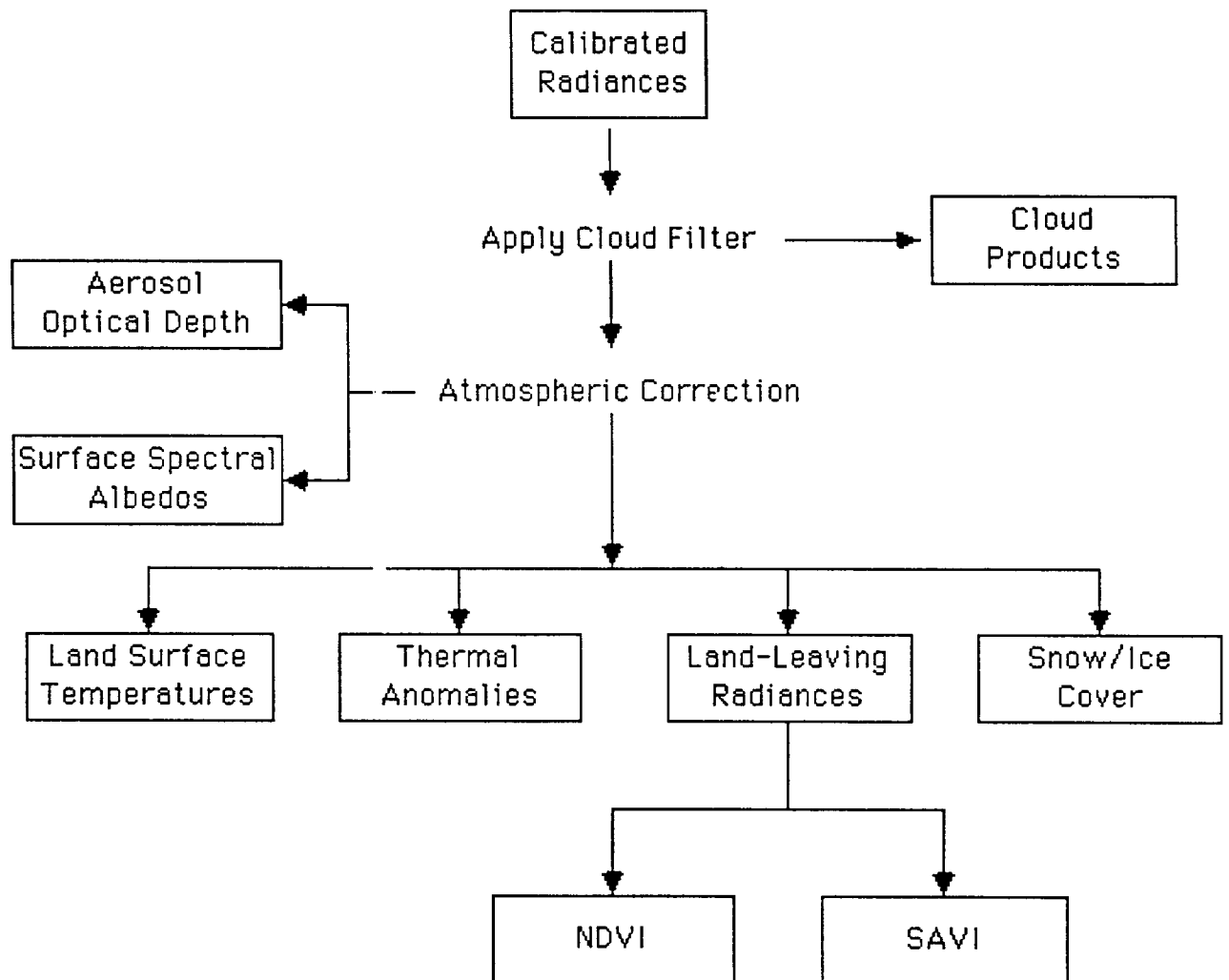
Except for Aerosol Optical Depth and Spectral Surface Albedo, the processing scheme shown in the following figure assumes that all atmospheric computations required to support land product processing are done as a part of atmospheric processing. Since Aerosol Optical Depth and Surface Spectral Albedo both affect the radiance observed by the MODIS instruments, they appear as simultaneous unknowns in the solution process, and Surface Spectral Albedo is obtained automatically as a coproduct of atmospheric correction. Surface Spectral Albedo might be computed in the final stage of atmospheric processing just before dedicated land processing begins.

The atmospherically corrected radiances serve as inputs for the determination of Land Surface Temperatures, Thermal Anomalies, vegetation indices, and Snow/Ice Cover. Since Thermal Anomalies (fires and volcanic eruptions) may affect the apparent value of the land surface temperature, Thermal Anomaly events may need to be tagged in the listings of Land Surface Temperature. Similarly, extraordinary values of Land Surface Temperatures may help to corroborate Thermal Anomaly events, so that apparent Land Surface Temperature may be examined as a part of the Thermal Anomaly identification process.

Snow/Ice identification also makes use of land temperature determinations. Pixels with a reflectance greater than 35% and a temperature below 0 degrees C are identified as snow/ice covered.

The vegetation indices may be obtained either for uncorrected or atmospherically corrected radiances. Atmospherically corrected indices are best for identifying long term trends and it will be assumed that these are desired for MODIS use. Since the computation of vegetation indices may be made to depend on the presence or absence of snow cover, the snow cover flag may serve as an input for the computation of vegetation indices.

MODIS Land Core Data Product Processing Scenario



Required MODIS Bands in the Ocean Core Data Products Scenario Preliminary

Below are listed the MODIS bands required to produce the ocean core data products based on the revised bands of Bill Barnes, October 25, 1989. These bands are divided into those requiring atmospheric correction to produce water-leaving radiances and those requiring water vapor correction to produce sea surface temperatures. The sea ice algorithm requires no atmospheric correction, and utilizes bands used for other ocean products, so it is not listed. This list is presented in an effort to define the preliminary ocean data processing scenario.

Table 1. MODIS-N bands requiring atmospheric correction for water-leaving radiance.

<u>Band</u>	<u>Product</u>
1. Band 9 (415 nm)	Gelbstoff/Case 2 Chlorophyll/ K_{PAR}
2. Band 10 (443 nm)	Chlorophyll/ K_{490}/K_{PAR}
3. Band 11 (490 nm)	Chlorophyll/ K_{PAR}
4. Band 12 (531 nm)	Chlorophyll/Aerosol Radiances/ K_{PAR}
5. Band 13 (565 nm)	Chlorophyll/Aerosol Radiances/ K_{490}/K_{PAR}
6. Band 14 (653 nm)	Atmospheric Correction/Aerosol Radiances/ Fluorescence/ K_{PAR} /Angstrom Exponents
7. Band 15 (681 nm)	Aerosol Radiances/Fluorescence/ K_{PAR}
8. Band 16 (745 nm)	Atmospheric Correction/Aerosol Radiances/ Angstrom Exponents
9. Band 17 (865 nm)	Atmospheric Correction/Aerosol Radiances

Total MODIS-N Bands = 9

Table 2. MODIS-N bands requiring water vapor correction for sea surface temperature.

1. Band 21 (3.75 μm)
2. Band 31 (11.03 μm)
3. Band 33 (12.02 μm)

Total MODIS-N Bands = 3

MODIS-T will not produce sea surface temperature or sea ice, but only water-leaving radiances and products derived therefrom. However, all of the bands in the visible wavelengths will probably be used for research, even if they are not required for core data products. Thus MODIS-T will require atmospheric correction for all of the bands between 400 and 700 nm.

Table 3. MODIS-T bands requiring atmospheric correction for water-leaving radiance.

<u>Band</u>	<u>Product</u>
1. Band 1 (410 nm)	Gelbstoff/Case 2 Chlorophyll/ K_{PAR}
2. Band 2 (425 nm)	Research/ K_{PAR}
3. Band 3 (440 nm)	Chlorophyll/ K_{490}/K_{PAR}
4. Band 4 (455 nm)	Research/ K_{PAR}
5. Band 5 (470 nm)	Research/ K_{PAR}
6. Band 6 (485 nm)	Chlorophyll/ K_{PAR}
7. Band 7 (500 nm)	Research/Aerosol Radiances/ K_{PAR}
8. Band 8 (515 nm)	Chlorophyll/Aerosol Radiances/ K_{PAR}/K_{490}
9. Band 9 (530 nm)	Research/Aerosol Radiances/ K_{PAR}
10. Band 10 (545 nm)	Chlorophyll/Aerosol Radiances/ K_{PAR}
11. Band 11 (560 nm)	Chlorophyll/Aerosol Radiances/ K_{PAR}
12. Band 12 (575 nm)	Research/Aerosol Radiances/ K_{PAR}
13. band 13 (590 nm)	Research/Aerosol Radiances/ K_{PAR}
14. Band 14 (605 nm)	Research/Aerosol Radiances/ K_{PAR}
15. Band 15 (620 nm)	Research/Aerosol Radiances/ K_{PAR}
16. Band 16 (635 nm)	Research/Aerosol Radiances/ K_{PAR}
17. Band 17 (650 nm)	Fluorescence/Aerosol Radiances/ K_{PAR}
18. Band 18 (665 nm)	Atmospheric Correction/Fluorescence/ Aerosol Radiances/Angstrom Exponents/ K_{PAR}
19. Band 19 (680 nm)	Fluorescence/Aerosol Radiances/ K_{PAR}
20. Band 20 (695 nm)	Fluorescence/Aerosol Radiances/ K_{PAR}
21. Band 21 (710 nm)	Fluorescence/Aerosol Radiances
22. Band 24 (755 nm)	Atmospheric Correction/Aerosol Radiances/ Angstrom Exponents
23. Band 31 (860 nm)	Atmospheric Correction/Aerosol Radiances/ Angstrom Exponents
or	
23. Band 32 (875 nm)	Atmospheric Correction/Aerosol Radiances/ Angstrom Exponents

Total MODIS-T Bands = 23

Sea Ice Determination by AVHRR as an Analogy to MODIS

Gesell, 1989 presents an algorithm using the channels available on the Advanced Very High Resolution Radiometer (AVHRR) to determine surface and cloud parameters. This procedure considers snow or sea ice covered pixels as contaminants of the cloud algorithm. Sea ice or snow covered pixels are flagged as cloudy by the AVHRR Processing scheme Over Land, cLOUD and Ocean (APOLLO) software. APOLLO is a software package developed at the United Kingdom's Meteorological Office. The algorithms use the five AVHRR channels (0.58 to 0.68 μm , 0.725 to 1.1 μm , 3.55 to 3.93 μm , 10.3 to 11.3 μm , and 11.5 to 12.5 μm) respectively and the differing spectral properties of sea ice, snow, and water at those wavelengths (Figure 1).

The snow and ice detection algorithms uses a threshold testing scheme based upon the wavelength and the desired parameter. Reflectances at 3.7 μm are used to distinguish between snow or sea ice covered pixels and cloudy pixels. Reflectances less than a threshold value can be tagged as snow or ice covered and cloud free. At 3.7 μm , clouds have much higher reflectivity. Additional testing is done to the pixel using the difference in reflectance between channel 1 and 2, (D_{12}).

The first two tests (R_{13} and D_{12}) identify pixels for further testing to determine if they are ice free. These tests use the channel 4 temperature, channel 1 and 2 reflectances, and temperature difference between channel 4 and 5.

The water emissivity is greater than sea ice emissivity in the 11.5 to 12.5 μm channel. In the 10.3 to 11.3 μm channel, the emissivity of sea ice and water are identical. This property is used to distinguish between sea ice and snow cover. The temperature difference between the two channels are greater over sea ice than over snow cover. This difference (D_{45}) is a function of the channel 4 and 5 temperature, the relative air mass through which the radiation passed, and the ocean's salinity.

The R_{21} test (in the sixth box down) determines if the ratio of the reflectances indicates the presence of sea ice. The remaining tests determine the presence of cloud free sea ice pixels or sea ice pixels under clouds. These threshold values used are shown in the appropriate boxes.

The snow cover algorithm has one test which applies to sea ice. A category snow-on-ice is chosen for an ocean pixel if the R_{31} test indicates it is snow contaminated.

This algorithm was tested during the 1987 Baltic Sea ice season. Only when thin ice clouds over snow, ice, or ice free water caused the classification of a few pixels to be uncertain. When it failed, it caused sea ice free pixels with thin ice clouds over water to be classified as sea ice covered. The

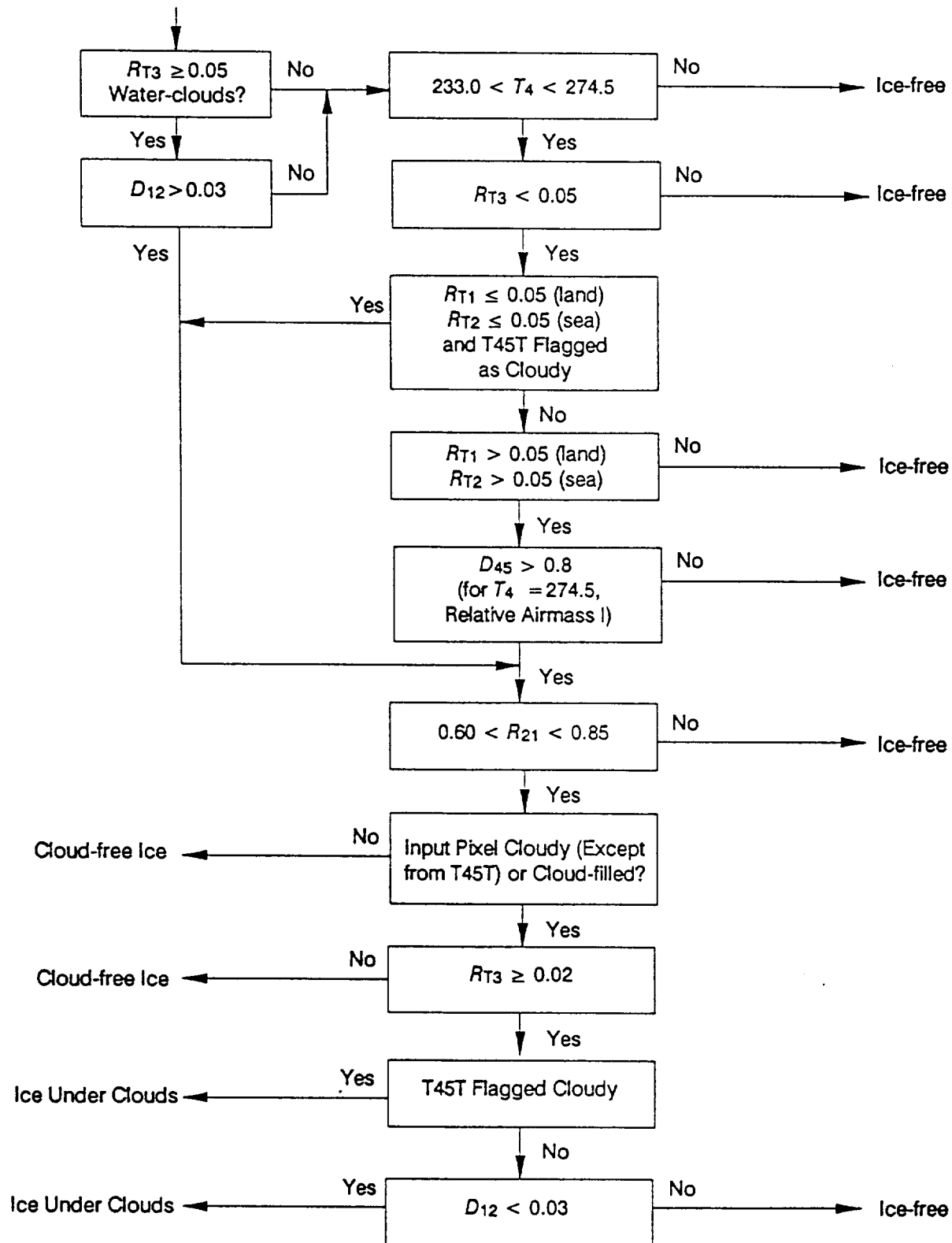
algorithm also fails to distinguish between thick, bright ice with a rough surface and when the snow is melting or frozen

Figure 1 symbols and their meanings are explained below.

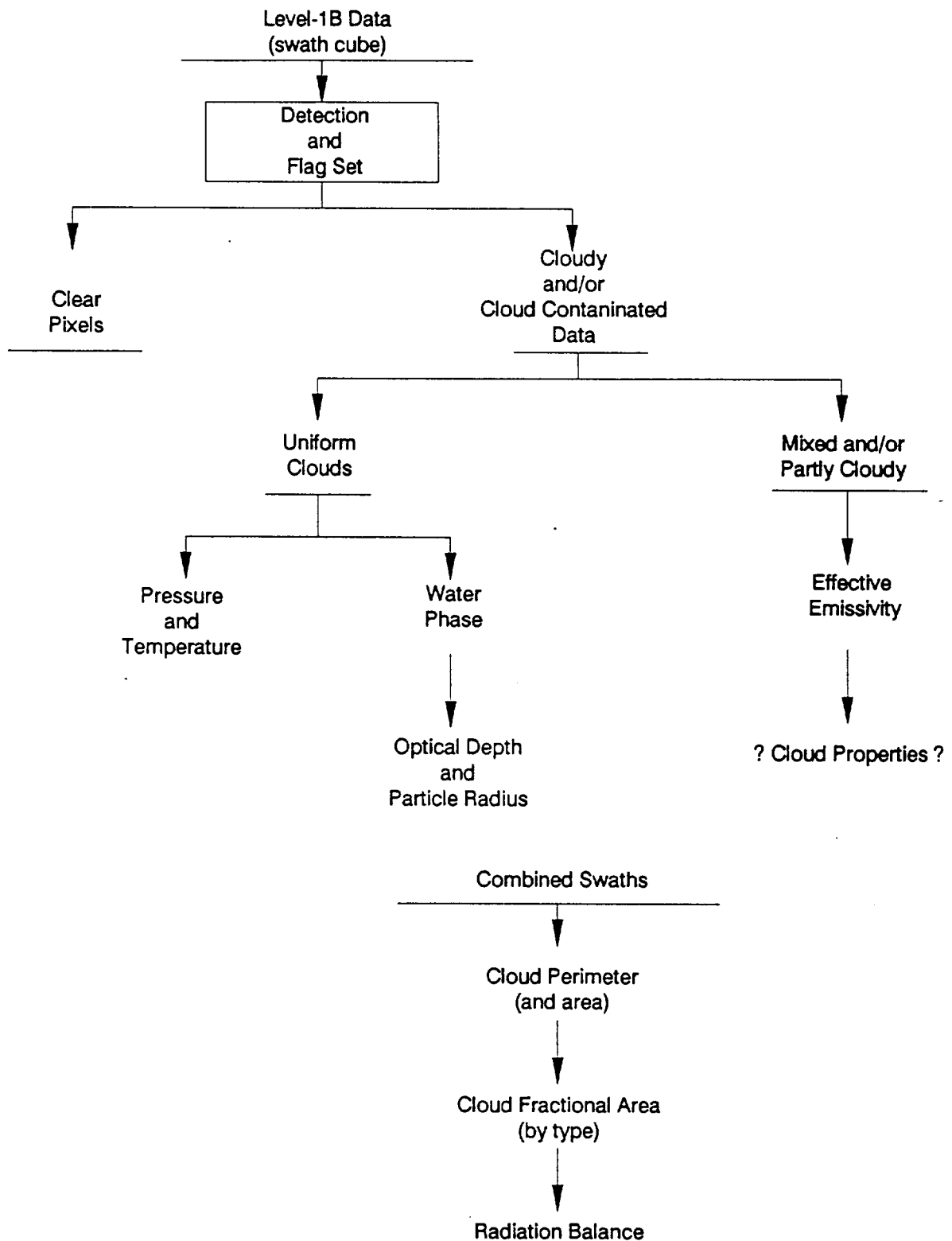
- o $R_{1,2,3}$ - Top of the atmosphere reflectances of channels 1, 2, and 3 respectively.
- o $T_{4,5}$ - Channel 4 and 5 temperatures °K
- o R_{21} - Ratio of reflectances of channel 2/ channel 1; i.e., R_{12}/R_{11}
- o D_{45} - Temperature difference between channel 4 and channel 5 in °K ;i.e., $T_4 - T_5$
- o R_{31} - Ratio of reflectances of channel 3/ channel 1; i.e., R_{13}/R_{11}
- o D_{12} - Difference of reflectances of channel 1 and channel 2 ;i.e., $R_{11} - R_{12}$
- o T45T - Temperature difference test between channels 4 and 5 This test detects sea ice as thin clouds.

REFERENCES:

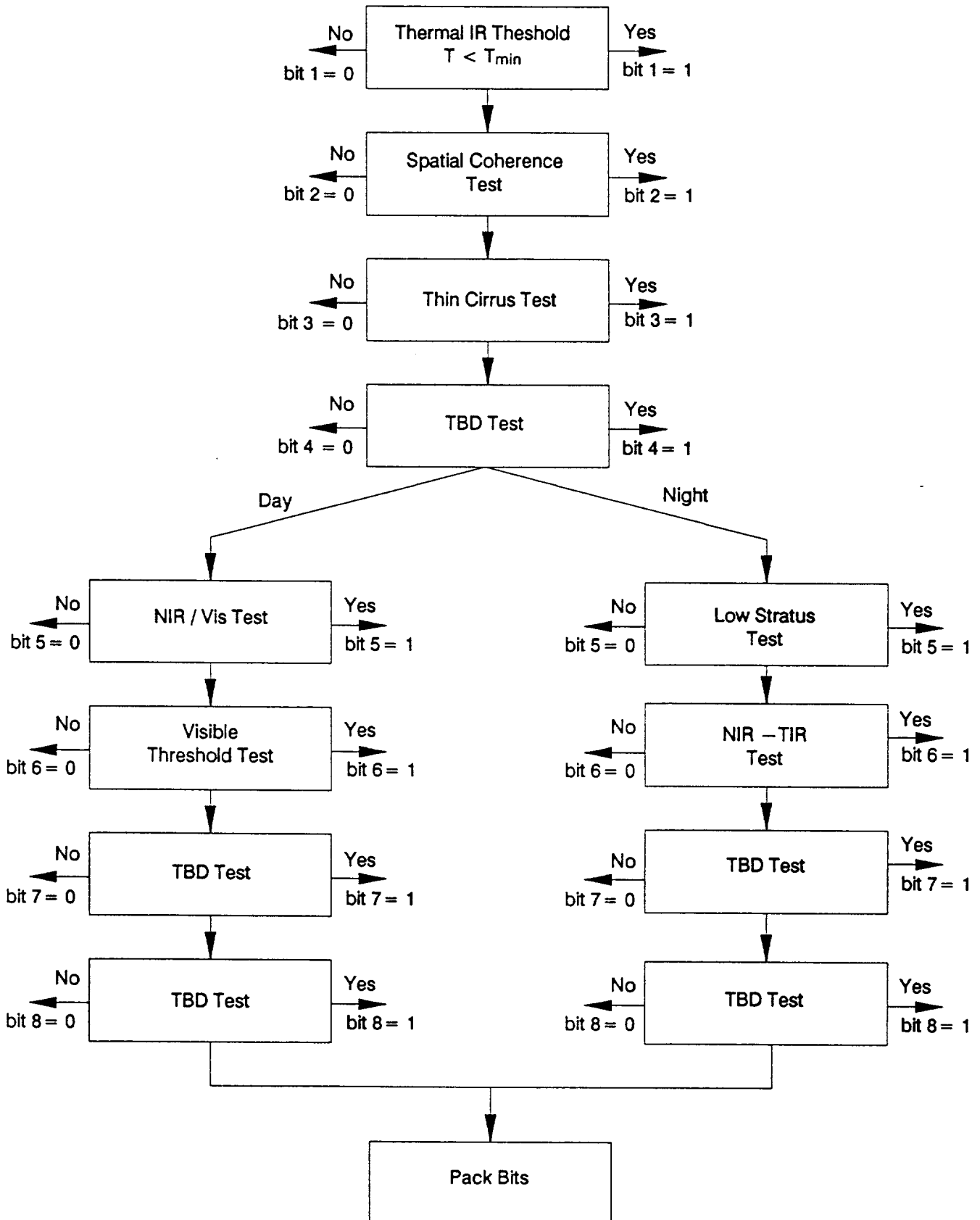
Gesell, G., An Algorithm for Snow and Ice Detection Using AVHRR Data: An Extension to the APOLLO Software Package. International Journal of Remote Sensing, Vol. 10, No.4 and 5 1989, pp 897 - 905.



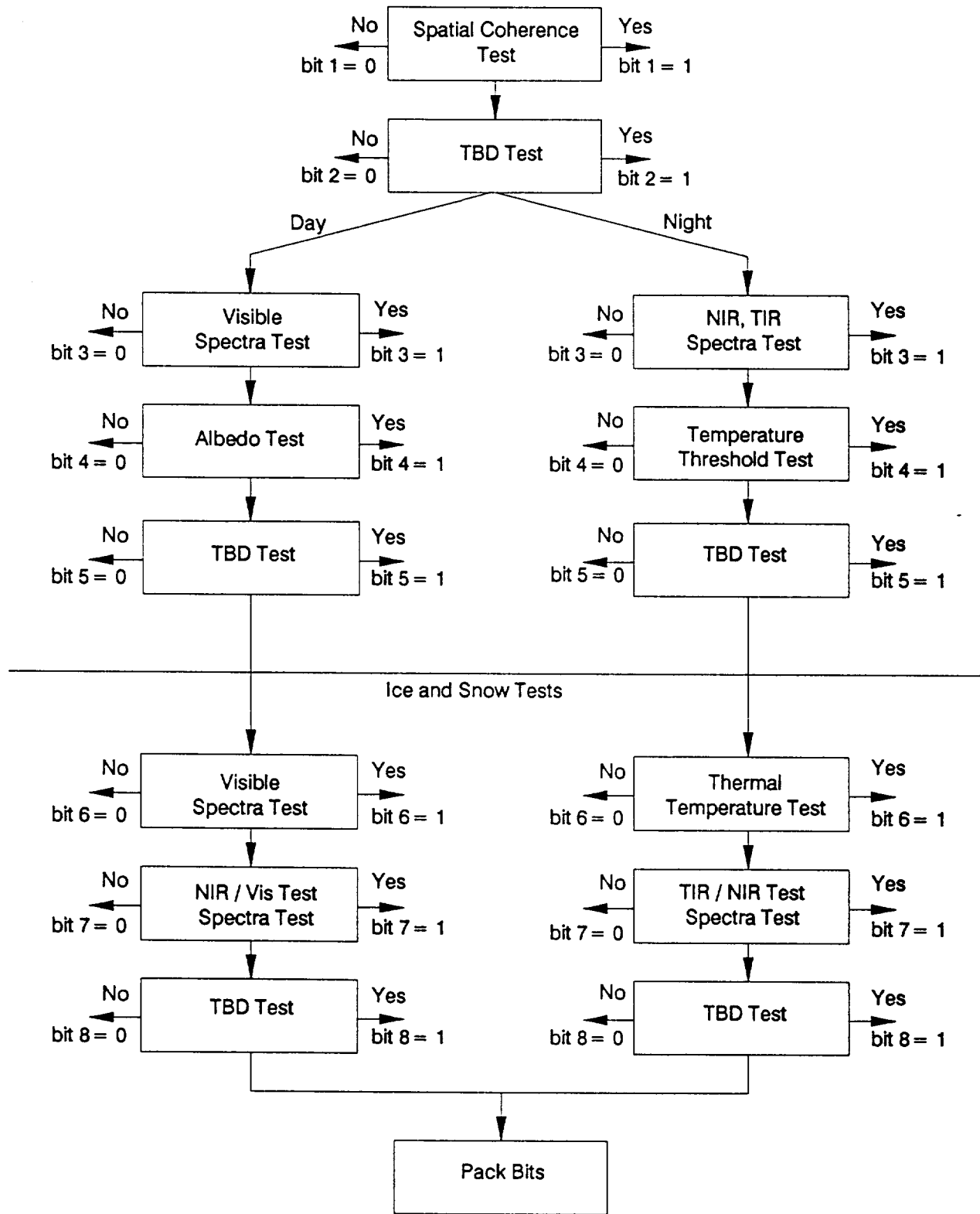
Cloud Products Overview



Cloud Flags
Part 1
Clear Pixel Identification



Cloud Flags
Part 2
Pixel Classification



Development of Model to Estimate MODIS-N Radiances

Based upon Bird, R. E. and C. Riordan, 1986: Simple solar spectral model for direct and diffuse irradiance on horizontal and tilted planes at the Earth's surface for cloudless atmospheres. J. Climate and Appl. Met., 25, 87-97.

Objectives:

Provide simple model to estimate MODIS radiances, for use in error analyses, diagnostic studies, etc.

Bird-Riordan model modified to give top of atmosphere radiances for clear and cloudy skies.

Model is on Lotus spreadsheet.

Input parameters:

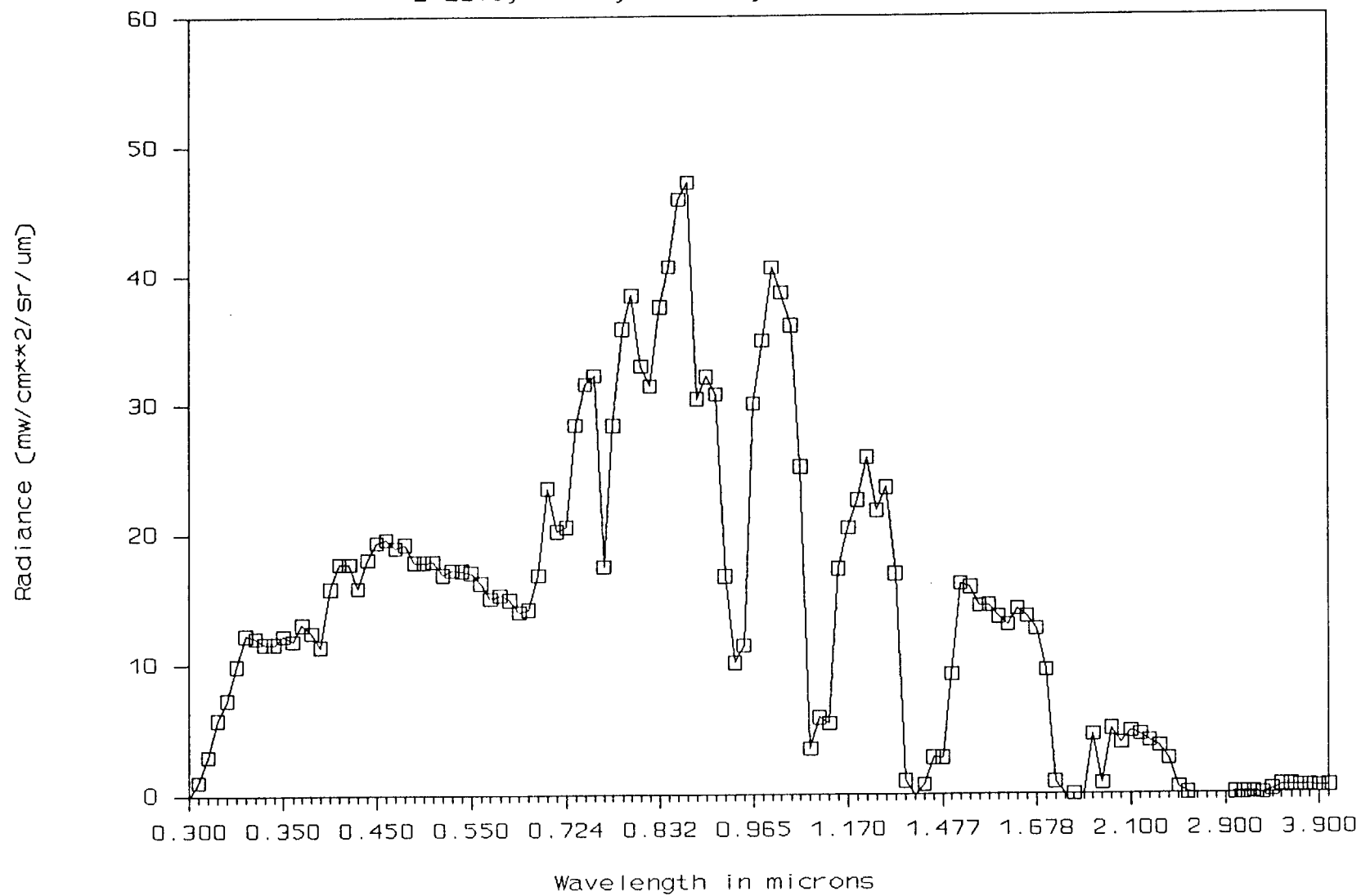
- 1) Solar zenith angle
- 2) Satellite zenith angle
- 3) Total ozone
- 4) Total precipitable water
- 5) Cloud droplet mean radius
- 6) Cloud droplet concentration
- 8) NDVI
- 9) Aerosol single scattering albedo
- 10) Day of year

Outputs:

- 1) Surface normal incidence spectral irradiances.
- 2) Surface horizontal direct, diffuse and total spectral irradiances.
- 3) Land leaving spectral irradiances.
- 4) Top of atmosphere spectral radiances.

Typical Modis Radiances over Land

$z=22.5, w=1.42, \rho_3=0.344, ndvi=0.53, b=.075$



PRELIMINARY ESTIMATES OF MODIS CORE DATA PRODUCT ACCURACIES, AND THEIR RELEVANCE TO KEY EARTH SCIENCE ISSUES		SCIENCE QUESTION ADDRESSED						ESTIMATED ACCURACY OF MODIS CORE DATA PRODUCT	
I. ATMOSPHERE CORE DATA PRODUCT ANALYSES		1	2	3	4	5	6	PRESENT-DAY	MODIS-ERA
A. <u>Total Column Ozone</u>		I					I	±5 to 10%	±5 to 10%
B. <u>Aerosol Optical Depth</u>		I	I				D	±.05	±.05
C. <u>Aerosol Size Distribution</u>		I	I				D	±10%	±10%
D. <u>Aerosol Mass Loading</u>		I	I				D	±40%	±30%
E. <u>Aerosol Single Scattering Albedo</u>		I	I				D	±.04	±.04
F. <u>Lifted Index</u>				D				±3°C	±3°C
G. <u>Temperature and Moisture Profiles</u>				I		I		±2°C	±1°C
H. <u>Total Precipitable Water</u>						D		±30%	±15%
I. <u>Cloud Fractional Area</u>		D		D	D			±10% absol.	±10% absol.
J. <u>Cloud Area and Perimeter</u>				D	D			±	±
K. <u>Cloud Optical Thickness</u>		D		D	D			±50% absol.	±20% absol.
L. <u>Cloud Effective Emissivity</u>				D	D			±20% absol.	±20% absol.
M. <u>Cloud Top Pressure</u>				D				±25 to 50mb	±25 to 50mb
N. <u>Cloud Top Temperature</u>				D				±2°C	±1°C
O. <u>Cloud Water Thermodynamic Phase</u>				D				N/A	Possible
P. <u>Cloud Droplet Effective Radius</u>				D				±10%	±10%
II. LAND CORE DATA PRODUCT ANALYSES		1	2	3	4	5	6	PRESENT-DAY	MODIS-ERA
A. <u>Vegetation Indices</u>			D			D		±0.1	±.04
B. <u>Surface Temperature</u>			D		D	D		±10C	±2°C
C. <u>Thermal Anomalies</u>			D			D		±50°C	±5°C
D. <u>Spectral Surface Albedo</u>					D	D		±.01	±.01
E. <u>Snowcover</u>					D			N/A	N/A
F. <u>Level-2 Land-Leaving Radiances</u>			I		I	I		±20%	±10%
G. <u>Level-1 Topographic Corrections</u>			I		I	I		±km	100m
H. <u>Surface Water Cover Mapping</u>						D		N/A	N/A
III. OCEAN CORE DATA PRODUCT ANALYSES		1	2	3	4	5	6	PRESENT-DAY	MODIS-ERA
A. <u>Sea Surface Temperatures</u>		D		D	D			±0.6K	±0.3K
B. <u>Sea Ice</u>		I			D			Yes, if 25%	Yes, if 25%
C. <u>Water Leaving Radiance</u>		D						±10%	±7%
D. <u>Chlorophyll Fluorescence</u>		D						N/A	±50 to 100%
E. <u>Chlorophyll-A Pigment Concentration</u>		D						±35%	±20%
F. <u>Case-II Waters Chlorophyll-A Pigment Concentration</u>		D						300%	±50%
G. <u>Detached Coccolith Concentration</u>		D						N/A	±35%
H. <u>Surface Incident Photosynthetically Active Radiation</u>		D						±40%	±25%
I. <u>Attenuation at 490nm</u>		D						±35%; R ² =0.9	±20%
J. <u>Attenuation of Photosynthetically Active Radiation</u>		D						N/A	±20%
K. <u>Primary Productivity</u>		D						R ² = 0.30	±?
L. <u>Angstrom Exponent</u>		I				D			
M. <u>Single Scattering Aerosol Radiation</u>		I				D		±10%	±6%
N. <u>In-situ Validation Observations</u>		I		I				Instr. Dep.	Instr. Dep.

Notes: "D" indicates that a science question/issue is directly addressed.
"I" indicates that a science question/issue is indirectly addressed.

Total Column Ozone

Total column ozone can be retrieved to an accuracy of 15 to 20 Dobson units using TOVS. The HIRS2/MSU retrieval has comparable accuracy and the AIRS/AMSU/MODIS retrievals should also have these accuracies. For a mean total column ozone level of 300 Dobson units, the expected systematic error is ± 5 to 10%.

Susskind, J., J. Rosenfield, D. Reuter, and M. T. Chahine, 1984. Remote sensing of weather and climate parameters from HIRS2/MSU on TIROS-N. *J. Geophys. Res.*, 89D, 4677-4897.

Ohring, G., K. Gallo, A. Gruber, W. Planet, L. Stowe, and J. D. Tarpley, 1989. Climate and global change: Characteristics of NOAA satellite data. *Eos*, 70, 889.

Aerosol Optical Depth

AVHRR retrievals of aerosol optical depth over oceans is ± 0.05 . Kaufman obtains similar uncertainties. The accuracies may be limited by various factors such as the limits on accuracies of radiative transfer models and the radiometer accuracies. It is not anticipated that the accuracies will improve markedly in the future.

News and Notes, 1989: AVHRR derived aerosol optical thickness products archived, *Bull. Amer. Meteor. Soc.*, 70, 1155.

Tanre, D., P. Y. Deschamps, C. Devaux, and M. Herman, 1988: Estimation of saharan aerosol optical thickness from blurring effects in thematic mapper data, *J. Geophys. Res.*, 93D, 15955-15964.

Aerosol Size Distribution

Spinhirne, J. D., and M. D. King, 1985: *J. Geophys. Res.*, 90C, 10,607.

Aerosol Mass Loading

Uncertainties in the aerosol mass loading arise from uncertainties in aerosol optical depth, aerosol single scattering albedo, the dependence on relative humidity, and uncertainties in the proportionality constant. The $\pm 40\%$ figure is given by Fraser et al.

Fraser, R. S., Y. J. Kaufman, and R. L. Mahoney, 1984: Satellite measurements of aerosol mass and transport, *Atmos. Environ.*, 18, 2577-2584.

Aerosol Single Scattering Albedo

Kaufman reports a derivation of aerosol single scattering albedo with an accuracy of ± 0.04 .

Kaufman, Y. J., 1987: Satellite sensing of aerosol absorption, *J. Geophys. Res.*, 92D, 4307-4317.

Lifted Index

Bolton, D., 1980: The computation of equivalent potential temperature, *Mon. Wea. Rev.*, 108, 1046-1053.

Temperature and Moisture Profiles

Satellite retrievals compared to radiosonde retrievals agree to ± 1 to ± 2 °C. MODIS retrievals should have comparable accuracies (there is an indication that AIRS/AMSU/MODIS retrievals will double the present accuracies).

Menzel, P., 1983: An evaluation of atmospheric soundings from geostationary satellites, Appl. Optics, 22, 2686.

Menzel, P., 1981: First sounding results from VAS-D, Bull. Amer. Meteor. Soc., 20, 3641.

Reuter, D., J. Susskind, and A. Pursh, 1988: First guess dependence of a physically based set of temperature-humidity retrievals from HIRS2/MSU data, J. Atm. Ocean. Tech., 5, 70-83.

Susskind, J., J. Rosenfield, and D. Reuter, 1983: An accurate radiative transfer model for use in the direct physical inversion of HIRS2 and MSU temperature sounding data, J. Geophys. Res., 88C, 8550-8568.

Total Precipitable Water

From AVHRR experience, a systematic error in retrieval of total precipitable water of $\pm 30\%$ is expected.

Ohring, G., K. Gallo, A. Gruber, W. Planet, L. Stowe, and J. D. Tarpley, 1989. Climate and global change: Characteristics of NOAA satellite data. Eos, 70, 889.

Reuter, D., J. Susskind, and A. Pursh, 1988: First guess dependence of a physically based set of temperature-humidity retrievals from HIRS2/MSU data. J. Atm. Ocean. Tech., 5, 70-83.

Cloud Fractional Area

The error should be 0.10. The determination becomes less accurate as the fractional coverage decreases.

Wielicki, B. A. and J. A. Coakley, Jr., 1981: Cloud retrieval using infrared sounder data: error analysis, J. Appl. Meteor., 20, 157.

Susskind, J., D. Reuter, and M. T. Chahine, 1987: Cloud fields derived from analysis of HIRS2/MSU sounding data, J. Geophys. Res., 92D, 4035-4050.

Cloud Area and Perimeter

Cloud Optical Thickness

This algorithm is expected to achieve accuracies of 3% for very thick uniform clouds. A more reasonable error estimate may be 0.2 in the optical depth estimate.

King, M. D., 1987: Determination of the scaled optical thickness of clouds from reflected solar radiation measurements, J. Atmos. Sci., 44, 1734.

Nakajima, T., and M. D. King, 1989: Determination of the optical thickness and effective particle radius of clouds from reflected solar radiation measurements. Part I: Theory, J. Atmos. Sci., in press.

Cloud Effective Emissivity

The error should be estimated as 0.20. The actual error will be a function of the measured value. The determination will be more accurate for larger values, i.e., the absolute error will be larger for small effective emissivity than for large effective emissivity.

Eyre, J. R., and W. P. Menzel, 1989: Retrieval of cloud parameters from satellite sounder data: a simulation study, J. Appl. Meteor., 28, 267.

Cloud Top Pressure

The error should be ± 50 mb. The accuracy increases for thicker clouds.

Wylie, D. P. and W. P. Menzel, 1989: Two years of cloud cover statistics using VAS, J. Climate, 2, 380.

Cloud Top Temperature

For sufficiently thick clouds, the temperature uncertainty is equivalent to the uncertainty in the thermal infrared brightness temperature. The uncertainties in pressure determination and profiles will determine the error for thinner clouds.

Wielicki, B. A. and J. A. Coakley, Jr., 1981: Cloud retrieval using infrared sounder data: error analysis, J. Appl. Meteor., 20, 157.

Cloud Water Thermodynamic Phase

Cloud Droplet Effective Radius

Nakajima, T., and M. D. King, 1989: Determination of the optical thickness and effective particle radius of clouds from reflected solar radiation measurements. Part I: Theory, J. Atmos. Sci., in press.

Vegetation indices

Estimated accuracy of NDVI is ± 0.1 presently, and ± 0.04 in the future for canopies such that the NDVI is greater than 0.2. When the NDVI is less than 0.2, the accuracy deteriorates. Specific accuracy estimates are not contained in the PIs' proposals. Reasonableness of the estimates are based on personal communications with Garrick Gutmann (NOAA/NESDIS) and Sam Goward (U of MD).

Estimated accuracy of SAVI is ± 0.025 at present.

Huete, A. R., 1988: A Soil-Adjusted Vegetation Index (SAVI), Remote Sensing of the Environment, 25, 295-309.

Surface temperature

Wan, Zhengming, Land Surface Temperature Measurements from Eos MODIS Data, Proposal Submitted to NASA, June 1988.

Thermal anomalies

Thermal Anomalies ± 50 °C at present, and ± 5 °C in the MODIS era.

Fires and other high temperature events very reliably detected--supporting references:

Kaufman, Yoram J., Global Monitoring of Aerosols Properties - Aerosol Climatology, Atmospheric Corrections, Biomass Burning, and Aerosol Effect on Clouds and Radiation, MODIS Team Member Proposal, June, 1988

Stephens, George, and Michael Matson, Regional and Global Fire Detection Using AVHRR Data, Presentation at the Twenty-First International Symposium on Remote Sensing of the Environment, Ann Arbor, Michigan, October 26-30, 1987.

Temperature accuracies are estimates for whole pixel scenes based on presently existing instruments and required MODIS capabilities and expected global surface temperature accuracy for normal, non-anomalous land surfaces.

Preliminary Specification for the Moderate-Resolution Imaging Spectrometer - Nadir (NADIR), GSFC-415-EOS-00006, Goddard Space Flight Center, Greenbelt, MD 21044, September 18, 1989

Spectral surface albedo

Kaufman, Y. J. and C. Sendra, 1988: Algorithm for automatic corrections to visible and near-IR satellite imagery, Int. J. Remote Sensing, 9, 1357-1381.

Kaufman, Y. J., 1988: Atmospheric effect on spectral signature - measurements and corrections, IEEE Trans. Geosciences and Remote Sensing, 26, 441-450.

Snowcover

Rossow, W. B., C. L. Brest, and L. C. Garder Global, 1989: Seasonal surface variations from satellite radiance measurements, J. Climate, 2, 214-247.

Rossow, W. B., L. C. Garder, and A. A. Lacis Global, 1989: Seasonal cloud variations from satellite radiance measurements, Part 1: sensitivity of analysis, J. Climate, 2, 419-458.

Level 2-Land Leaving Radiances

Level-1 Topographic Corrections

Surface Water-Cover Mapping

Sea Surface Temperatures

On present algorithms, the RMS accuracy is on the order of 0.6 K relative to drifting buoys.

McClain, E. P., W. G. Pichel, and C. C. Walton, 1985: Comparative performance of AVHRR-based multichannel sea surface temperatures, J. Geophys. Res., 90, 11,587-11,601.

Barton, 1985: Transmission Model and Ground-Truth Investigation of Satellite-Derived Sea Surface Temperatures. J. Clim. Appl. Met., 24, 508-516.

Future instruments are being designed to provide SST accuracies to 0.3K.

Barton, I. J., A. M. Zavody, D. M. O'Brien, R. W. Saunders, and D. T. Llewellyn-Jones, 1989: Theoretical Algorithms for Satellite-Derived Sea Surface Temperatures. J. Geophys. Res., 94, 3365-3375.

G. Ohring et.al., Trans. Amer. Geophys. U., 70, October 10, 1989.

Sea Ice

Can unambiguously determine the presence of sea-ice if the pixel is at least 25% sea-ice covered.

Rosow, W. B., L. C. Garder, and A. A. Lacis, 1989: Global, seasonal cloud variations from satellite radiance measurements, Part 1: sensitivity of analysis. J. Climate, 2, 419-458.

Water Leaving Radiance

Gordon, H. R., D. K. Clark, J. W. Brown, O. B. Brown, R. H. Evans, and W. W. Broenkow, 1983: Phytoplankton pigment concentrations in the Middle Atlantic Bight: comparison of ship determinations and CZCS estimates, Applied Optics, 22, 20-36.

Chlorophyll Fluorescence

The accuracies are about $\pm 100\%$ when chlorophyll-a concentrations are low, and about $\pm 50\%$ when chlorophyll-a concentrations are high.

Gower, J. F. R. and G. A. Borstad, 1987: On the use of the solar-stimulated fluorescence signal from chlorophyll a for airborne and satellite mapping of phytoplankton, Advances in Space Research, 7, 101-106.

Chlorophyll-A Pigment Concentration

Gordon, H. R., D. K. Clark, J. W. Brown, O. B. Brown, R. H. Evans, and W. W. Broenkow, 1983: Phytoplankton pigment concentrations in the Middle Atlantic Bight: comparison of ship determinations and CZCS estimates, Applied Optics, 22, 20-36.

Assuming improvement due to the validation program of D.K. Clark.

Case-II Waters Chlorophyll-A Pigment Concentration

Carder, K. L. 1989: High spectral resolution MODIS-T algorithms for ocean chlorophyll in Case II waters, Eos Team Member Proposal.

Detached Coccolith Concentration

The accuracy is ± 2700 cells/ml (out of a maximum observed value of 9000 cells/ml) when reflectances are the independent variable using a linear regression. The accuracy is ± 0.03 (in fractional reflectance) when cells per milliliter are the independent variable. For the algorithm to work, the presence of coccoliths must first be identified through the diagnosis of "excess scattering."

Holligan, P. M., M. Viollier, D. S. Harbour, P. Camus, and M. Champagne-Philippe, 1983: Satellite and ship studies of coccolithophore production along a continental shelf edge, Nature, 304, 339-342.

Surface Incident Photosynthetically Active Radiation

Present errors are 21 Wm_{-2} RMS at local noon for both clear and cloudy conditions.

Kuring, N., M. R. Lewis, T. Platt, and J. E. O'Reilly, 1989: Satellite-derived estimates of primary productivity on the northwest Atlantic continental shelf, Continental Shelf Research, 89, in press.

Expected MODIS-era errors are 13 Wm_{-2} RMS at local noon for both clear and cloudy conditions, based on the expectation that MODIS algorithms will perform as well as GOES, using the Gautier and Katsaros model.

Gautier, C. and K. B. Katsaros, 1989: Insolation during STREX: Part I, comparisons between surface measurements and satellite estimates, J. Geophys. Res., 89, 11,779-11,788.

Attenuation at 490nm

$R^2=0.91$ (based on dependent data)

Austin, R. W. and T. J. Petzold, 1983: The determination of the diffuse attenuation coefficient of sea water using the Coastal Zone Color Scanner, In Oceanography from Space, J.F.R. Gower, ed., 239-256.

This algorithm is based on the determination of chlorophyll, so its accuracy is dependent upon the chlorophyll retrieval accuracy, which is expected to improve with MODIS.

Gordon, H. R., D. K. Clark, J. W. Brown, O. B. Brown, R. H. Evans, and W. W. Broenkow, 1983: Phytoplankton pigment concentrations in the Middle Atlantic Bight: comparison of ship determinations and CZCS estimates, Applied Optics, 22, 20-36.

Attenuation of Photosynthetically Active Radiances

This algorithm is based on the determination of chlorophyll, so its accuracy is dependent upon the chlorophyll retrieval accuracy.

Primary Productivity

Balch, W. M., M. R. Abbott, and R. W. Eppley, 1989: Remote sensing of primary production--I, A comparison of empirical and semi-analytical algorithms, Deep-Sea Research, 36, 281-295.

Angstrom Exponent

Single Scattering Aerosol Radiances

Gordon, H. R., D. K. Clark, J. W. Brown, O. B. Brown, R. H. Evans, and W. W. Broenkow, 1983: Phytoplankton pigment concentrations in the Middle Atlantic Bight: comparison of ship determinations and CZCS estimates, Applied Optics, 22, 20-36.

Gordon, H. R. and D. J. Castano, 1989: Aerosol analysis with the coastal zone color scanner: a simple method for including multiple scattering effects, Applied Optics, 28, 1320-1326.

In-situ Validation Observations

The in-situ observations are derived from moored and drifting buoys, and include physical, biological, and optical instruments and measurements.

Clark, D. K., 1988: Marine Optical Characterization, Proposal for NASA in response to AO# OSSA-1-88.

External Data Sets, External Look-Up Tables,
and Internal Data Sets
Required for MODIS Ocean Data Processing

Listed below are the external data sets, external look-up tables, and internal data sets required for the data processing scenario for ocean products, and the corresponding core data products they are required for. An external data set is a set of variables obtained outside the MODIS processing environment that vary as a function of time and space. They are thus required for each MODIS position and time. An external look-up table is a fixed data set comprised of constants that do not change for location and space. The look-up table may either be a set of constants that are used directly in the processing scenario, or may require input variables which are then used to produce other variables necessary for data processing. The inputs may be internal or external variables, but are used in the tables to interpolate in pre-specified variable dependencies. Internal data sets are those variables produced within the MODIS processing scenario that are used more than once in the processing. This list applies both to the MODIS-N as well as the MODIS-T processing scenarios.

External Data Sets

Core Product

- | | |
|-------------------------------------|--|
| 1. Atmospheric Surface Pressure | Water-Leaving Radiance
(Rayleigh Radiance) |
| 2. Surface Wind Speeds | Water-Leaving Radiance
(Sun Glitter Correction) |
| 3. Spectral Ozone Optical Thickness | Water-Leaving Radiance
(Ozone Correction) |

External Look-Up Tables

- | | |
|---|--|
| 1. Mean Extraterrestrial Solar
Spectral Irradiance | Water-Leaving Radiance
Aerosol Radiances
Angstrom Exponents
K_{PAR} |
| 2. Spectral Rayleigh Optical Thickness
at Standard Temperature, Pressure | Water-Leaving Radiance
(Rayleigh Radiance) |

- | | |
|---|---|
| 3. Fourier Coefficients of Rayleigh Scattering (function of Rayleigh optical thickness, solar zenith angle, spacecraft zenith angle) | Water-Leaving Radiance (Rayleigh Radiance) |
| 4. Fresnel Reflectance for Downwelling Irradiance, Upwelling Irradiance | K_{PAR} |
| 5. Seawater Index of Refraction | K_{PAR} |
| 6. Empirical Constants for <ul style="list-style-type: none"> - chlorophyll - K_{490} - possibly coccoliths - primary production | Chlorophyll a
K_{490}
Detached Coccoliths
Primary Production |
| 7. Backscattering Coefficients <ul style="list-style-type: none"> - chlorophyll for Case 1 waters - chlorophyll and other substances for Case 2 waters | K_{PAR} |
| 8. Case 2 Gelbstoff-Chlorophyll Table (function of ratio $L_w(410)/L_w(443)$ and ratio $L_w(443)/L_w(565)$) | Case 2 Chlorophyll |

Internal Data Sets Used More Than Once

1. Pixel Latitude and Longitude
2. Spacecraft Pitch, Roll, Yaw
3. Solar Zenith Angle
4. Solar Azimuth Angle
5. Spacecraft Zenith Angle
6. Spacecraft Azimuth Angle
7. Instantaneous Extraterrestrial Solar Spectral Irradiance
8. Instantaneous Extraterrestrial Solar Spectral Irradiance Corrected for Ozone Absorption
9. Rayleigh Optical Thickness

In addition to the above data sets required for MODIS processing, in-situ validation products will be generated from ships and buoys. These data will be processed through EosDIS and require a separate scheme for data handling and access. The data products are listed below.

- | | |
|-----------------------------|-------------------------|
| 1. Ships of opportunity and | Sea surface temperature |
|-----------------------------|-------------------------|

drifting buoys (Brown, Barton, Carder, Abbott, Esaias)	Primary production
2. Optical buoys (Clark)	Water leaving radiance Downwelling irradiance Upwelling irradiance K_{PAR} Chlorophyll Total suspended matter Phaeopigments
3. Australian project (Parslow)	Water-leaving radiance Chlorophyll Sea surface temperature Biological, chemical, and Physical Properties
4. AOL (Hoge)	Chlorophyll Chlorophyll Fluorescence